Journal of Natural Fibers

ISSN: 1544-0478 (Print) 1544-046X (Online) Journal homepage: www.tandfonline.com/journals/wjnf20

Structural, Morphological and Thermal Properties of Kenaf Microcrystalline Cellulose/Poly (Butylene Adipate-Co-Terephthalate) Films for Packaging Applications

Aatikah Meraj, Ahmad Safwan Ismail & Mohammad Jawaid

To cite this article: Aatikah Meraj, Ahmad Safwan Ismail & Mohammad Jawaid (2025) Structural, Morphological and Thermal Properties of Kenaf Microcrystalline Cellulose/Poly (Butylene Adipate-Co-Terephthalate) Films for Packaging Applications, Journal of Natural Fibers, 22:1, 2455978, DOI: 10.1080/15440478.2025.2455978

To link to this article: https://doi.org/10.1080/15440478.2025.2455978

JOURNAL OF NATURAL FIBERS
2025, VOL. 22, NO. 1, 2455978
https://doi.org/10.1080/15440478.2025.2455978

Taylor & Francis
Taylor & Francis Group

Structural, Morphological and Thermal Properties of Kenaf Microcrystalline Cellulose/Poly (Butylene Adipate-Co-Terephthalate) Films for Packaging Applications

Aatikah Meraj[a], Ahmad Safwan Ismail[b], and Mohammad Jawaid[c]

[a]Laboratory of Bio-polymer and its Derivatives, Institute of Tropical Forestry and Forest Products (INTROP) Universiti Putra Malaysia, Serdang, Malaysia; [b]Laboratory of Bio composite Technology, Institute of Tropical Forestry and Forest Products (INTROP) Universiti Putra Malaysia, Serdang, Malaysia; [c]Department of Chemical and Petroleum Engineering, United Arab Emirates University (UAEU), Al Ain, United Arab Emirates

ABSTRACT

The aim of this work is to use microcrystalline cellulose (MCC), obtained from kenaf fibers by using eutectic green solvents, to build compostable packaging films by adding them to Poly (butylene adipate-co-terephthalate) (PBAT). In this study, microcrystalline cellulose was incorporated into PBAT composites through melt-mixing, followed by hot pressing at 130°C. PBAT and MCC were produced in various formulations (0.5, 1, 1.5 wt%) to enhance and sustain inherent characteristics of films. The structural, morphological, thermal, and tensile properties of PBAT and microcrystalline cellulose film were examined using X-ray Diffraction, Scanning electron microscope (SEM), Thermal analysis, and Universal Testing Machine. The uniform dispersion of MCC within the PBAT matrix significantly contributes to improved thermal stability, as evidenced by delayed degradation, and enhanced heat resistance. SEM makes it evident that addition of MCC to PBAT influences the surface morphology, with an optimal range promoting mechanical adherence through roughness. However, excessive MCC content leads to imperfections such as cavities, potentially compromising material performance. The inclusion of MCC content enormously raised the tensile modulus of the PBAT/MCC film, increasing its stiffness while tensile strength decreased on addition of MCC in PBAT/MCC formulations. Cellulose film could potentially be used as a biodegradable film in food packaging applications.

摘要

这项工作的目的是使用微晶纤维素（MCC），通过使用共晶绿色溶剂从红麻纤维中获得，通过将其添加到聚己二酸丁二醇酯-共对苯二甲酸酯（PBAT）中来构建可堆肥的包装薄膜. 在这项研究中，微晶纤维素通过熔融混合掺入PBAT复合材料中，然后在130°C下热压. PBAT和MCC以各种配方（0.5、1、1.5重量%）生产，以增强和维持薄膜的固有特性. 使用X射线衍射、扫描电子显微镜（SEM）、热分析和万能试验机检查了PBAT和微晶纤维素薄膜的结构、形态、热和拉伸性能. MCC在PBAT基质中的均匀分散显著有助于提高热稳定性，这可以通过延迟降解和增强耐热性来证明. SEM表明，在PBAT中添加MCC会影响表面形态，最佳范围通过粗糙度促进

KEYWORDS
Microcrystalline cellulose; biodegradable; tensile properties; Packaging; poly (butylene adipate-co-terephthalate)

关键词
微晶纤维素; 能进行生物降解的; 拉伸性能; 包装聚己二酸丁二醇酯

CONTACT Mohammad Jawaid jawaid@uaeu.ac.ae Department of Chemical and Petroleum Engineering, College of Engineering, United Arab Emirates University (UAEU), Al Ain, United Arab Emirates

Present affiliation for Ahmad Safwan Ismail is Chemical Engineering Programme, Faculty of Engineering, Universiti Malaysia Sabah, Jalan UMS, 88400, Kota Kinabalu, Sabah, Malaysia

机械粘附. 然而，过多的MCC含量会导致诸如空腔等缺陷，从而可能损害材料性能. MCC含量的加入极大地提高了PBAT/MCC薄膜的拉伸模量，增加了其刚度，而在PBAT/MMC配方中添加MCC后，拉伸强度降低. 纤维素薄膜有可能在食品包装应用中用作可生物降解的薄膜.

Introduction

Today’s world depends significantly on polymeric materials, which are currently used in wide range of industries, namely aerospace, aeronautics, agrifood, medical science, automobiles, medicine, sensors, etc (Arico et al. 2005; Huang et al. 2003; Krebs 2009; Stuart et al. 2010; Vargas Ferreira et al. 2016). Polyethylene, Polypropylene, Polystyrene, and Poly(vinyl chloride) are most extensively used and accessible common plastics (Mohanty, Misra, and Hinrichsen 2000). These polymers are the most widely generated, used, and found plastics in the environment. As a result, they represent one of the most troublesome groups of solid wastes, having detrimental effects on soil and water. Due to their benign effects, biodegradable polymers provide a lot of benefits for environmental preservation. This has a direct connection to how resistant they are to deterioration caused by environmental factors like humidity and microbial attack. Swapping out non-biodegradable polymers for biodegradable ones is a way to address these environmental issues (Ikada and Tsuji 2000; Rezwan et al. 2006; Siracusa et al. 2008).

The most promising, biodegradable, well-known aliphatic-aromatic co-polyester polymer with enormous future potential in wide range of applications is Polybutylene adipate-co-tere-phthalate; abbreviated as PBAT. It is produced by polycondensation of butanediol, adipic acid, and terephthalic acid and this mixture has proven great characteristics and excellent biodegradability. It also has excellent mechanical qualities due to the aromatic unit in molecular chain and has properties comparable to those of low-density polyethylene (LDPE) (Jian, Xiangbin, and Xianbo 2020). The ductility and flexibility of PBAT are comparable to LDPE, its biodegradability makes an excellent substitute to many packaging films (Barbosa, Souza, and Rosa 2020). PBAT is the most often used polymer for biodegradable plastic film bags, owing its outstanding toughness, flexibility, low elastic modulus, and exceptional heat resistance (Bai et al. 2021). But its widespread applicability is constrained, nonetheless, by its cost and weak tensile strength.

To overcome these limitations, researchers have explored incorporating renewable fillers like Microcrystalline Cellulose (MCC) into polymer matrices. MCC is widely utilized in numerous applications, including those in medicine, cosmetics, food, etc (Kumar, de la Luz Reus-Medina, and Yang 2002; Petersson and Oksman 2006). In addition, the use of plant sources, namely, MCC (Pandian et al. 2023), starch (Ma et al. 2017), and proteins (Tchmutin et al. 2004), etc enhances the biodegradability of the films. MCC are preferred reinforcing filler in the polymer blend over alternative fibers because of its low price, nontoxic nature, relatively low density, renewable, and biodegradability. The biodegradable substance MCC can be used along with PBAT. As MCC is purified cellulose which when combined with appropriate biodegradable polymer PBAT will not only improve tensile properties but also reduce the overall costs which enhance biodegradability of packaging film. Therefore, the usage of biodegradable packaging films including PBAT, and their combination with MCC can be widely used to combat plastic film.

Several studies have investigated the integration of MCC into biodegradable polymer blends. In a recent study by (Sinsukudomchai et al. 2023), a biocomposite film was prepared by combining polyhydroxy butyrate (PHB) along with esterified MCC from pineapple leaves as fillers, and the results demonstrated acceptable tensile strength, tensile modulus and minor increase in elongation at break which can improve flexibility. Unlike previous studies that used MCC derived from conventional sources, this work explores the potential of MCC derived from kenaf fibers using green eutectic solvents, a sustainable extraction method. PBAT as filler used to create compostable packaging films.

Three different formulations i.e., 0.5%, 1%, and, 1.5% PBAT/MCC were prepared by melt mixing in Brabender followed by hot press for compostable film. The chemical, thermal and morphological characteristics were examined by Fourier transform infrared spectroscopy, thermogravimetric analysis, and scanning electron microscopy respectively. Tensile properties of PBAT/MCC films were also investigated. The crystallization properties of the PBAT/MCC were also characterized. The result obtained PBAT/MCC films can be utilized as potential compostable film for food packaging, leveraging innovative materials and methods to address persistent environmental challenges.

Materials and methods

Materials

Poly butylene adipate-co-tere-phthalate (PBAT) a biodegradable polymer with molecular weight of 1.42×10^5 g/mol and 1.24–1.26 g/cm^3 density, under the trade name Ecoflex, a product of BASF used as the polymer matrix. MCC was isolated from kenaf fiber biomass pre-treated with natural deep eutectic solvents (NADES). Prior to obtaining MCC, the kenaf fiber underwent a bleaching process with 10% sodium chlorite solution, followed by drying, and was then subjected to acidic hydrolysis to isolate KF-MCC particles, as detailed in our previous work (Meraj et al. 2023).

Methods

Fabrication of PBAT/MCC film

Firstly, the proportions of PBAT and MCC were separately weighed, as shown in Table 1, and dried overnight in an oven at 60°C. Sample was mixed into melt mixer (Brabender mixer) at 130°C for approx. 6 min with rotation of 50 rpm. After cooling the mixture, the sample was crushed by using Melchers crusher machine to get uniform pellets size i.e., mesh size 2 mm. Secondly, the prepared pellets were placed on steel plate with dimensions of 300 mm × 300 mm × 0.20 mm. The steel plate with sample was transferred to preheated hot press set at 130°C and subjected to a pressure of 30 tonnes for 12 minutes. After 12 min, the sample was transfer to cooling for 1 min. Lastly, different formulations (0.5, 1, and 1.5 wt%) of PBAT/MCC films prepared separately, were gently removed from the steel plate and sample obtained with a thickness of 0.20 mm which was subjected to further testing and tensile properties.

Characterisation and testing

Fourier transform infrared spectroscopy

FTIR was carried out using Perkin Elmer 1600 Infrared spectrometer, conducting 32 scans with 650–4000 cm^{-1} range of wavenumber at a resolution of 4 cm^{-1}. Samples were first crushed, then potassium bromide pellet was used to pelletize them to prepare samples for examination.

Thermal analysis

A thermogravimetric analyzer (TA Instruments Q500) was used to perform thermal examination of samples. In N_2 gas atmosphere, samples were scanned and heated from ambient temperature to 900°C at rate of 10°C min^{-1} in alumina cruicible. DSC was performed using TA instrument Q20 differential

Table 1. Shows experimental composition of PBAT/MCC film.

Name of Samples	PBAT wt%	MCC wt%
Pure PBAT	100	0
0.5% PBAT/MCC	99.5	0.5
1% PBAT/MCC	99	1
1.5% PBAT/MCC	98.5	1.5

scanning calorimeter. A heat rate of 10°C min^{-1} under N_2 atmosphere, approximately 5 mg of sample placed in alumina crucible was subjected to heat from ambient temperature to 430°C.

X-ray diffraction

Using Shimadzu X-ray diffractometer, model XRD6000, using Cu K radiation and a 2 hz scanning rate, the crystalline structure of fibers was examined and X-ray patterns of samples were obtained.

Scanning electron microscope and energy dispersive X-ray (EDX)

Morphological examination of samples was examined by using JEOL Model JSM 6400, Japan at different magnifications. The samples were mounted one by one on Al stub and sputter-coated with gold using Baltec SCD sputter coater, before analyzing the samples under the SEM instrument. Following that, an EDX spectrometer (Oxford Instruments, UK) was used to observe elemental composition and content of PBAT/MCC film samples.

Tensile properties

The mechanical test was performed using AI-3000, GOTECH Universal Testing Machine according to American Society for Testing and Materials (ASTM) D882. The experiment was carried out at crosshead speed of 12.5 mm min^{-1} with gauge length of 125 mm and maintaining a width of 20.005 mm in all samples. An average of the four tested samples outcomes was determined.

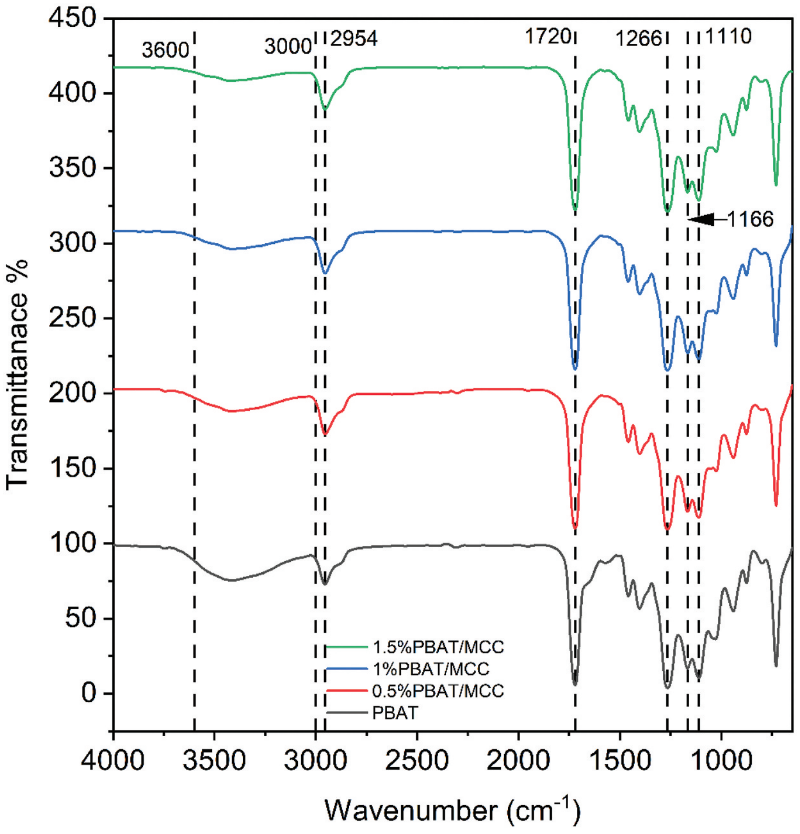

Figure 1. FTIR spectra of PBAT and 0.5, 1, and 1.5 wt. % of PBAT/MCC films.

Results and discussion

FTIR Analysis

FTIR spectroscopy was examined to characterize chemical composition of PBAT and PBAT/MCC (0.5, 1, and 1.5 wt%) films as shown in Figure 1. The FTIR spectra obtained broad absorption band ranging 3000–3600 cm^{-1} which corresponds to -OH stretching vibration and strong inter and intramolecular hydrogen bonding (Pavia, Lampman, and Kriz 2001). The PBAT/MCC films exhibits distinctive C-H stretching vibration at 2954 cm^{-1} indicating C-H stretching bonds between MCC and PBAT. Furthermore, peak at 1720 cm^{-1} corresponds to stretching of C=O ester group signaling characteristic peak of both PBAT and PBAT/MCC films. Absorption peak at 1266 cm^{-1} attributes to C–O stretching of carbonyl group conjugated with phenyl group. Similarly, absorption band at 1166 cm^{-1} and 1110 cm^{-1} corresponds antisymmetric bridge stretching of C – O and C – O – C pyranose ring vibration of cellulose and C-O-C stretching vibration of ester respectively (Giri et al. 2019, 2021; Wang et al. 2008). Absorption peak at 876 cm^{-1} attributes common cellulose structure that corresponds stretching vibration of C-O-C for β-1,4-glycosidic linkages (Wu 2012). Lastly, it was observed that FTIR spectra of 0.5, 1, and 1.5 wt. % of PBAT/MCC were almost identical to the PBAT spectrum, indicating that only H-bond interactions must have occurred between the components.

Thermal analysis

The TG curve shown in Figure 2. indicates difference in thermal degradation behavior of PBAT with varying percentages of MCC i.e.; 0.5, 1, and 1.5 wt. % of PBAT/MCC films. TGA was performed to

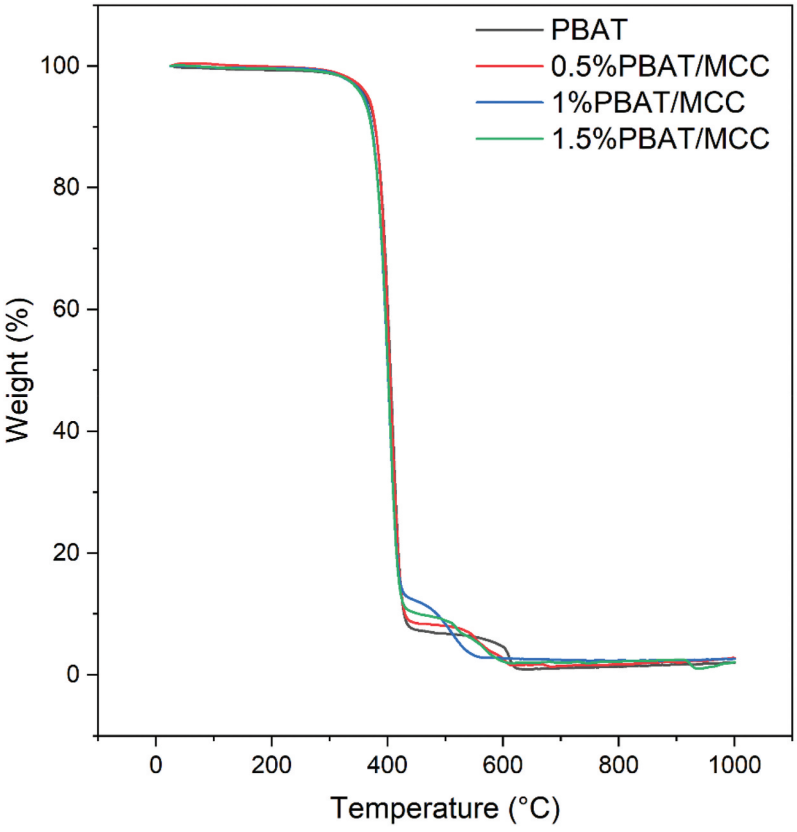

Figure 2. TG curves of PBAT and 0.5, 1, and 1.5 wt% of PBAT/MCC films.

investigate thermal stability of MCC as filler to PBAT for compostable packaging films. The initial weight loss was observed at temperatures ranging from 30°C to 150°C which is associated with the evaporation of moisture content and other volatile components present (Kian et al. 2022; Nagata and Inaki 2011; Sellami et al. 2019), followed by major degradation at temperature approx. 350°C. However, two step degradation was observed. The first degradation step occurs between approximately 200–400°C. This step corresponds to the thermal degradation of MCC and the less thermally stable components in the PBAT matrix, such as amorphous regions or additives. Whereas, second degradation step occurs between 400°C and 600°C, which is primarily associated with the decomposition of the PBAT polymer backbone. Furthermore, complete degradation of PBAT/MCC occurs at 460°C leaving behind a larger amount of residual (wt%) at 625°C in form of char after combustion. It was found that PBAT has lesser char residue, while it increases on further adding MCC to PBAT, due to lower thermal stability than PBAT. TGA results demonstrate that the PBAT/MCC films exhibit enhanced thermal stability compared to neat PBAT due to the incorporation of MCC as a filler. Thermal resistance, particularly in the range of 200–400°C, ensures that the films can withstand typical food packaging processes such as exposure to moderate heat during storage and handling. Therefore, thermogravimetric measurements enable the assessment of the heat resistance of the PBAT/MCC polymer films within the matrix. Table 2 shows the exhibited degradation process in a single step, and the parameters of their thermal stability.

DTG curves determine the weight loss and the precise temperature at which material degradation occurs. The thermal analysis of a combination of PBAT, and PBAT/MCC at different formulations with varying MCC content shown in Figure 3. As demonstrated in Figure 3. thermal degradation temperature increased, hence the thermal stability also increased. Furthermore, DTG curve of PBAT and PBAT/MCC exhibited a similar degradation pattern of a single peak in a one-step-degradation process. From Figure 3. highest peak temperature was observed in 1.5 wt% PBAT/MCC that is about 408.56°C. It was concluded that 1.5 wt% PBAT/MCC formulation was more thermally stable then PBAT.

On the other hand, DSC plot shows the thermal behaviors of PBAT, PBAT/MCC are shown in Figure 4a and summarized in Table 3. These peaks rise and fall irregularly to some degrees by the increase in MCC content to the PBAT/MCC formulations from 0.5 to 1.5 wt%. The peaks show disorder in the structure. From Figure 4(a), T_g value varies with addition of MCC. However, it was observed that T_m value of PBAT is 124.3°C which is approximately similarly observed in all the samples except 1.5% PBAT/MCC. Furthermore, the highest ΔH was observed in 1.5 wt% MCC i.e., 15.67 j/g at 260°C, and the least ΔH was observed at 315°C i.e., 0.80 j/g. Whereas 0.5 wt% MCC showed the largest exothermic peak i.e., 16.28 j/g at 290°C as compared to 1.5 wt% MCC. Furthermore, the temperature ranging from 110°C to 160°C, each sample of PBAT/MCC showed two endothermic peaks as shown in Figure 4(b), which attributes the insertion of MCC particles to the PBAT polymer (Zuo et al. 2017). Furthermore, the pronounced peaks in the range 200–300°C as shown in Figure 4(c), indicates thermal events associated with PBAT and PBAT/MCC films. These peaks likely correspond to the oxidative degradation or recrystallization processes occurring due to the interaction between PBAT and MCC. The neat PBAT sample shows a broad peak indicating its thermal stability and degradation onset compared to the PBAT/MCC films, whereas the peaks shift or intensify based on the MCC concentration. Additionally, the appearance of fourth and fifth exothermic peaks observed with addition of MCC and their shifts to higher

Table 2. TGA results of PBAT and 0.5, 1, 1.5 wt% of PBAT/MCC films.

Name of sample	Onset temperature (°C)	Degradation temperature (°C)	End set temperature (°C)	Residual (wt%)
PBAT	373.42	408.01	624.65	0.2909
0.5% PBAT/MCC	373.17	407.17	615.90	0.2611
1% PBAT/MCC	371.60	407.72	596.82	0.2971
1.5% PBAT/MCC	373.33	408.56	536.33	0.1801

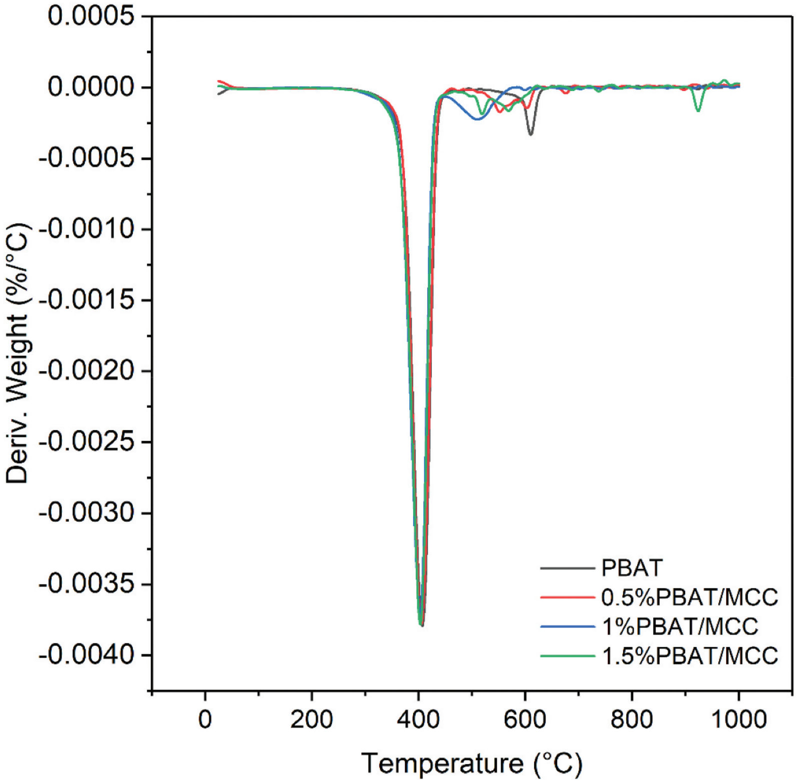

Figure 3. DTG curves of PBAT, PBAT/MCC films.

temperatures i.e., 250–330°C, which is ascribed to creation of H-bonds between polymer matrix and MCC (Lang et al. 2022).

SEM-EDX analysis

Surface morphology of PBAT shown in Figure 5(a) and PBAT/MCC films with 0.5%, 1%, and 1.5% wt% formulations are shown in Figure 5(b–d). The lower magnification of PBAT micrograph in Figure 5(a) demonstrates that there are areas that show both substantially smoother and rougher textures. Further, it can be seen in Figure 5(b–d), MCC was dispersed within the PBAT matrix and was observed by adding and increasing the MCC content i.e., 0.5%, 1%, and 1.5 wt% in PBAT/MCC film. As we moved further, it was found that, an increase in MCC content, topology of surface becomes rougher and cave-like structure can be seen in Figure 5(d). Moreover, when the addition is not excessive, the MCC's roughness helps to promote effective mechanical adherence (Lang et al. 2022; Mathew, Oksman, and Sain 2005). Furthermore, increasing MCC content in the PBAT matrix causes cavities and displays holes, resulting in imperfection, and becomes rougher as shown in Figure 5(c,d) (Botta et al. 2021; Lang et al. 2022).

Figure 6(e–h) displays spectra of PBAT and PBAT/MCC formulations at 0.5, 1, and 1.5 wt% and elemental composition in Table 4. It shows the changes in the element composition which indicates noticeable peaks for O and C elements. Some minute traces of other elements were also seen.

XRD analysis

Figure 7 depicts the results of the analysis of the PBAT/MCC crystalline structures using the X-ray diffraction technique. Three diffraction angles correspond to the 2θ at 23.7°, 44.1° and 64.3° which are

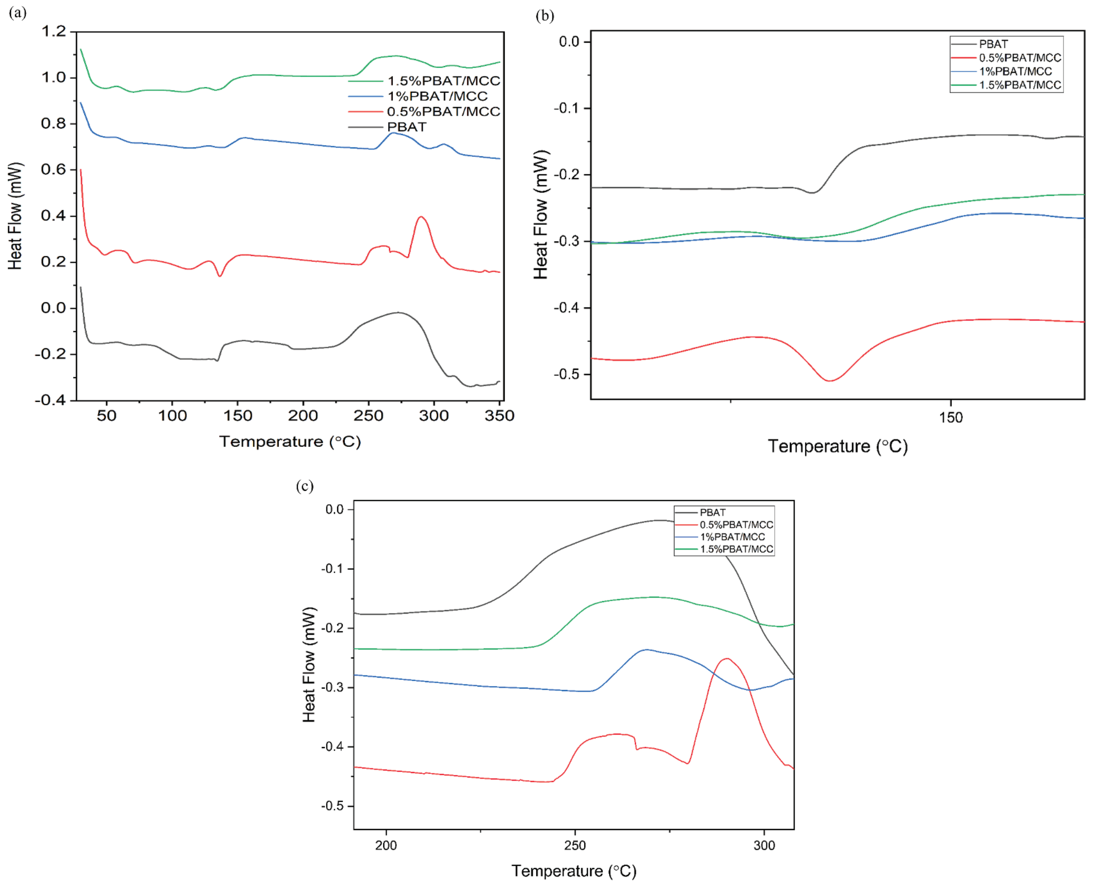

Figure 4. a. DSC plot of PBAT, PBAT/MCC films. b. Zoomed plot of PBAT, PBAT/MCC films. c. Enlarged part of DSC curves ranging from 200°C to 300°C of PBAT, PBAT/MCC films.

Table 3. Thermal behaviours of PBAT, PBAT/MCC films.

Name of sample	T_g (°C)	T_m (°C)	ΔH_1 (jg^{-1})	ΔH_2 (jg^{-1})	ΔH_3 (jg^{-1})	ΔH_4 (jg^{-1})	ΔH_5 (jg^{-1})
PBAT	68.62	124.3	−0.89	−15.21	73.49	-	-
0.5% PBAT/MCC	70.83	124.45	−2.21	−2.32	−4.29	10.05	16.28
1% PBAT/MCC	66.69	125.84	−0.49	−1.30	−1.78	8.57	2.52
1.5% PBAT/MCC	68.90	120.45	−1.37	−0.82	−2.30	15.67	0.80

observed in PBAT and PBAT/MCC films. The distinctive diffraction angles of crystalline structure of PBAT are represented by the peaks located at 23.7° (Olivato et al. 2013; Raquez et al. 2008). The PBAT crystalline peak overlaps the $2\theta = 22.5$ where the cellulose diffraction angle is meant to be exhibited (Reis et al. 2014). From Figure 7. it was observed that there is a weak crystalline diffraction peak. Whereas, with the addition of the MCC at 0.5, 1, and 1.5 wt. % the peak intensity and the crystalline quality of the PBAT/MCC film increases which could be due to more cellulosic materials present than that of pure PBAT. According to a study, Tessema, T. A. et. al., cellulose gains crystallinity through delignification and acid hydrolysis, which removes amorphous regions (Tessema et al. 2023). In another study, composites with 4% MCC exhibited the highest crystallinity index. Since, MCC is inherently crystalline, its addition to the composite naturally enhances the overall crystallinity of the material (Raharjo, Salam, and Ariawan 2023). However, in this PBAT/MCC films the addition of MCC improves the crystalline alignment and structure

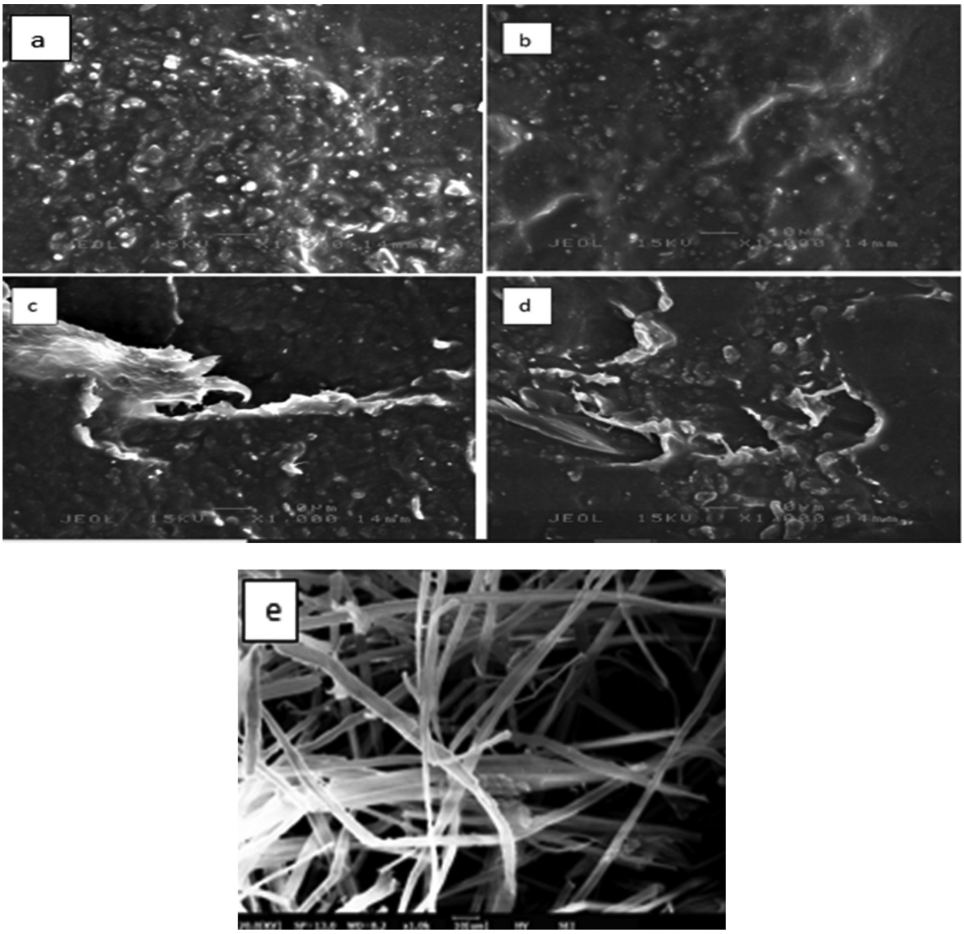

Figure 5. SEM micrographs of (a) PBAT, and (b-d) 0.5, 1, and 1.5 wt% of PBAT/MCC films, (e) SEM image of MCC.

of PBAT. In addition, MCC incorporation into PBAT enhances film crystallinity and material properties through its cellulosic crystalline structure. Thus, this suggests that the crystalline structure of the cellulose fibers, when present in enormous amount, increases the crystallinity of the films.

Tensile properties

Figure 8–10 depicts the impact of MCC loading on tensile characteristics of pure PBAT and PBAT/MCC films. From Figures 8 and 9, it was observed that tensile strength and tensile modulus respectively, tensile strength decreased when compared to pure PBAT and on addition of MCC decreased in PBAT/MCC formulations. This decrease may be related to the substantial addition of MCC which results in stiffness as compared to the pure PBAT, also due to poor dispersion generated by MCC aggregates in PBAT matrix due to weak contact between phases (Rasheed et al. 2021).

Whereas, from Figure 9 it was observed rigidity i.e., represented by tensile modulus which increased with an increase in MCC loading and is almost similar in 1 and 1.5 wt% of MCC/PBAT film. The cause of this phenomenon can be attributed due to production of MCC's network structure above the level of percolation through hydrogen bond interactions (Azizi Samir, Alloin, and Dufresne 2005; Reis et al. 2017; Sun et al. 2014). According to Ibrahim et al., strengthening effect of MCC fiber causes young modulus to increase while tensile strength did not enhance or even decreased which is similar to this study (Ibrahim, El-Zawawy, and Nassar 2010). A similar study was also reported by Ma

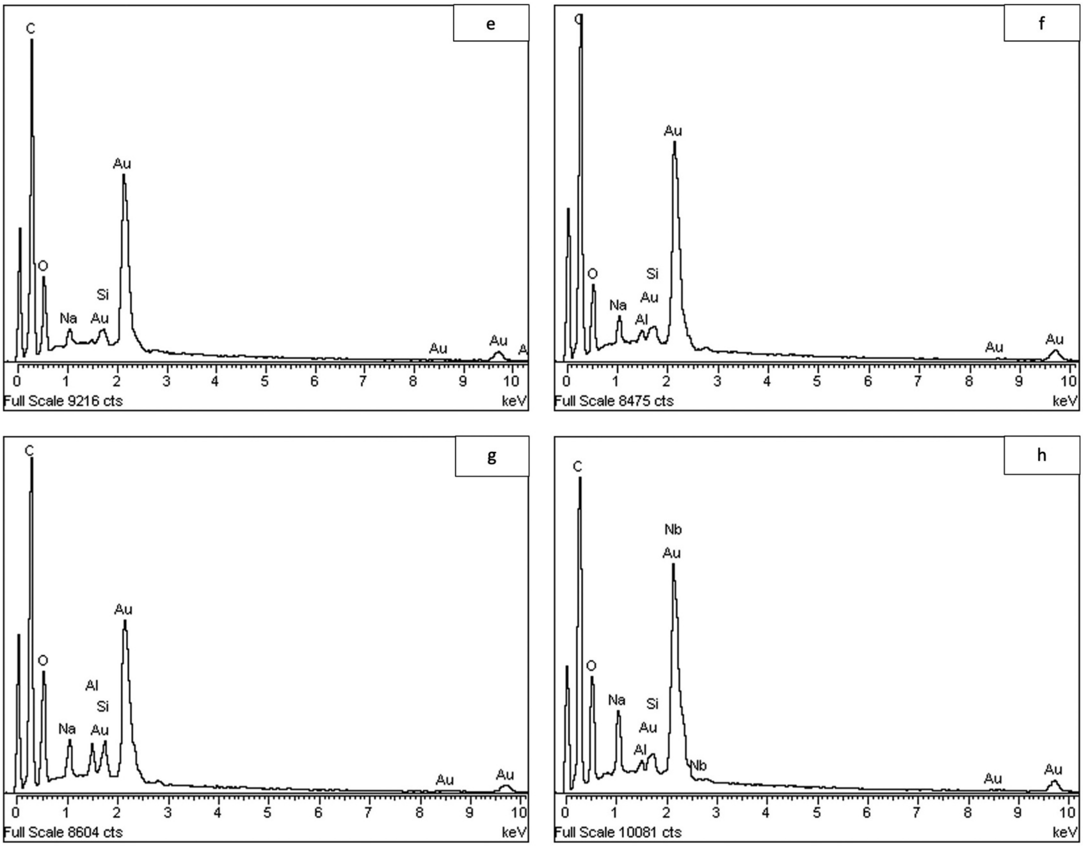

Figure 6. Figure 6 (e-h) displays the EDX spectra of PBAT and PBAT/MCC at 0.5, 1, and 1.5 wt. %.

Table 4. Summary of the elemental composition of PBAT and PBAT/MCC films.

Element	PBAT	0.5% MCC	1% MCC	1.5% MCC
	Wt. %	***Wt. %***	***Wt. %***	***Wt. %***
C	62.23	64.69	57.63	56.10
O	34.85	30.56	35.11	30.37
Na	1.81	2.82	3.05	4.64
Al	-	0.91	2.09	0.56
Si	1.11	1.02	2.12	0.74
Zn	-	-	-	-
Nb	-	-	-	7.59

et al. (Ma, Chang, and Yu 2008), for thermoplastic pea starch composites containing 12 wt% of MCC. Additionally, Mathew et al. (Mathew, Oksman, and Sain 2005), found that higher concentration of MCC decreases tensile strength and elongation at break while enhancing young modulus.

The elongation at break of PBAT/MCC shown in Figure 10. It shows elongation at break decreases with addition of MCC in PBAT/MCCfilms. This could be due to addition of MCC into PBAT matrix which did not result in significant improvement and showed a substantial decrease in elongation break. Haafiz et al. (Haafiz et al. 2013) studied that introducing MCC into a PLA matrix decreased the tensile mechanical properties i.e., tensile strength and elongation when compared to pure PLA. Although tensile modulus shows an increase in this property with the addition of MCC. In another study by Ries MO et al. (Reis et al. 2017), by increasing MCC concentration, there was a reduction in

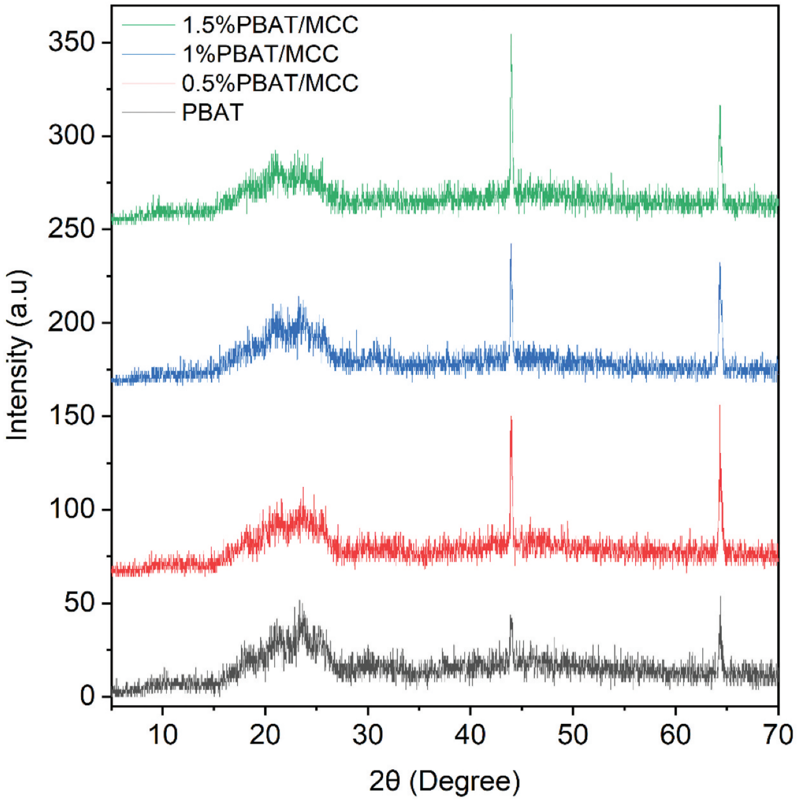

Figure 7. XRD patterns of PBAT, PBAT/MCC films.

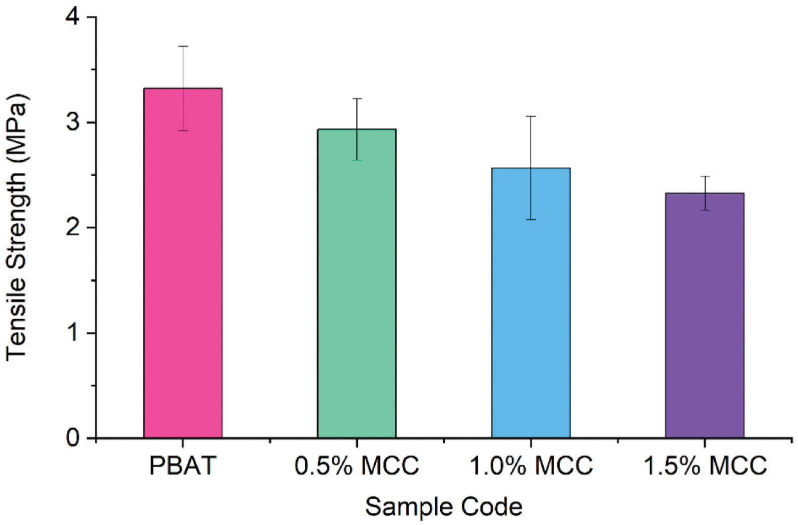

Figure 8. Tensile strength of PBAT and PBAT/MCC films.

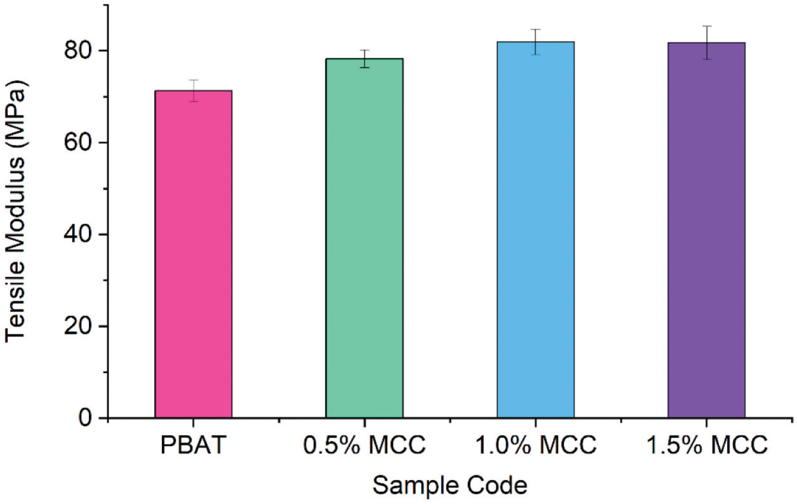

Figure 9. Tensile modulus of PBAT and PBAT/MCC films.

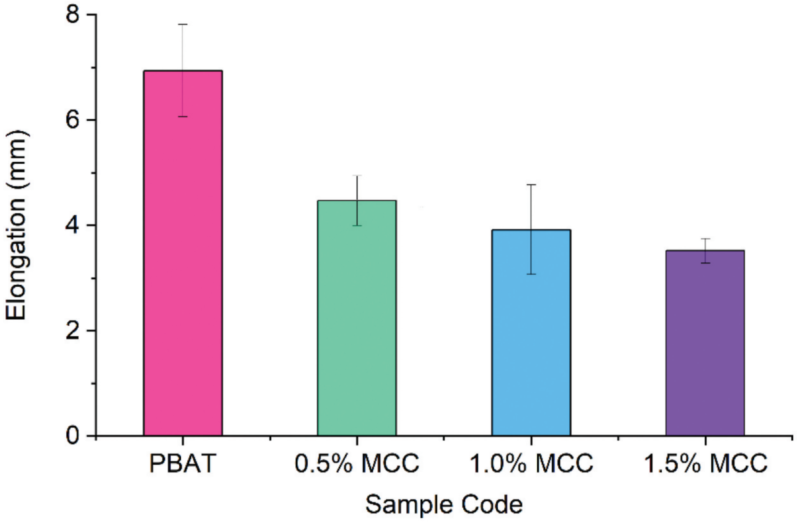

Figure 10. Shows elongation of PBAT and PBAT/MCC films.

elongation at break. Undoubtedly, materials have degrading properties which cannot be sacrificed in order to improve its mechanical capabilities. Therefore, the effect of MCC can change based on polymer matrix, the amount used, and the fabrication process.

Conclusion

An increasing amount of individuals have grown interested in biodegradable films because of the serious environmental issues caused by the careless use of conventional plastic films. PBAT based biodegradable films have the potential to provide several advantages for the environment and its biodegradability. In this study, four different formulations of 0.5, 1, and 1.5 wt. % MCC/PBAT were prepared and were successfully produced using microcrystalline cellulose obtained from kenaf fibers. The results of the findings of FTIR, SEM-EDX, and XRD analysis showed the PBAT/MCC better performance and good compatibility at 1.5 wt% PBAT/MCC. Scanning electron microscopy makes it evident that addition of microcrystalline cellulose to Poly (butylene adipate-co-terephthalate) influences the surface morphology, with an optimal range promoting mechanical adherence through roughness. However, excessive MCC content leads to imperfections such as cavities, potentially compromising material performance. The uniform dispersion of MCC within the PBAT matrix significantly contributes to improved thermal stability, as evidenced by delayed degradation, and enhanced heat resistance. Tensile modulus of PBAT/MCC film was increased with the addition of MCC content resulting in the stiffness of PBAT/MCC film, although tensile strength decreased in the samples. Thus, produced PBAT/MCC film has the potential to be used as a compostable film for food packaging purposes.

Disclosure statement

No potential conflict of interest was reported by the author(s).

Funding

We are thankful to the Universiti Putra Malaysia for funding this work under Putra Grant-[GP-IPS/2021/9698100]. The authors are also thankful to United Arab Emirates University for supporting this work by Fund Code; [12N233].

ORCID

Ahmad Safwan Ismail http://orcid.org/0000-0001-9062-0657

Highlights

- MCC within PBAT matrix significantly contributes to improved thermal stability.
- Addition of MCC significantly increase tensile modulus of PBAT/MCC films improving stiffness.
- In SEM, Addition of MCC enhanced surface roughness promoting mechanical adherence.
- Produced PBAT/MCC film potentially be used as biodegradable film in food packaging applications.

References

Arico, A. S., P. Bruce, B. Scrosati, J.-M. Tarascon, and W. Van Schalkwijk. 2005. “Nanostructured Materials for Advanced Energy Conversion and Storage Devices.” *Nature Materials* 4 (5): 366–377. https://doi.org/10.1038/nmat1368.

Azizi Samir, M. A. S., F. Alloin, and A. Dufresne. 2005. “Review of Recent Research into Cellulosic Whiskers, Their Properties and Their Application in Nanocomposite Field.” *Biomacromolecules* 6 (2): 612–626. https://doi.org/10.1021/bm0493685.

Bai, J., H. Pei, X. Zhou, and X. Xie. 2021. “Reactive Compatibilization and Properties of Low-Cost and High-Performance PBAT/Thermoplastic Starch Blends.” *European Polymer Journal* 143:110198. https://doi.org/10.1016/j.eurpolymj.2020.110198.

Barbosa, R. F., A. G. Souza, and D. S. Rosa. 2020. “Acetylated Cellulose Nanostructures as Reinforcement Materials for PBAT Nanocomposites.” *Polymer Composites* 41 (7): 2841–2854. https://doi.org/10.1002/pc.25580.

Botta, L., V. Titone, M. C. Mistretta, F. P. La Mantia, A. Modica, M. Bruno, F. Sottile, and F. Lopresti. 2021. “PBAT Based Composites Reinforced with Microcrystalline Cellulose Obtained from Softwood Almond Shells.” *Polymers* 13 (16): 2643. https://doi.org/10.3390/polym13162643.

Giri, J., R. Lach, W. Grellmann, M. A. B. H. Susan, J. M. Saiter, S. Henning, V. Katiyar, and R. Adhikari. 2019. “Compostable Composites of Wheat Stalk Micro- and Nanocrystalline Cellulose and Poly(butylene Adipate- Co -Terephthalate): Surface Properties and Degradation Behavior.” *Journal of Applied Polymer Science* 136 (43): 48149. https://doi.org/10.1002/app.48149.

Giri, J., R. Lach, H. H. Le, W. Grellmann, J.-M. Saiter, S. Henning, H.-J. Radusch, and R. Adhikari. 2021. “Structural, Thermal and Mechanical Properties of Composites of Poly (Butylene Adipate-Co-Terephthalate) with Wheat Straw Microcrystalline Cellulose.” *Polymer Bulletin* 78 (9): 4779–4795. https://doi.org/10.1007/s00289-020-03339-5.

Haafiz, M. M., A. Hassan, Z. Zakaria, I. M. Inuwa, M. S. Islam, and M. Jawaid. 2013. “Properties of Polylactic Acid Composites Reinforced with Oil Palm Biomass Microcrystalline Cellulose.” *Carbohydrate Polymers* 98 (1): 139–145. https://doi.org/10.1016/j.carbpol.2013.05.069.

Huang, Z., Y. Zhang, M. Kotaki, and S. Ramakrishna. 2003. “A Review on Polymer Nanofibers by Electrospinning and Their Applications in Nanocomposites.” *Composites Science and Technology* 63 (15): 2223–2253. https://doi.org/10.1016/S0266-3538(03)00178-7.

Ibrahim, M. M., W. K. El-Zawawy, and M. A. Nassar. 2010. “Synthesis and Characterization of Polyvinyl Alcohol/Nanospherical Cellulose Particle Films.” *Carbohydrate Polymers* 79 (3): 694–699. https://doi.org/10.1016/j.carbpol.2009.09.030.

Ikada, Y., and H. Tsuji. 2000. “Biodegradable Polyesters for Medical and Ecological Applications.” *Macromolecular Rapid Communications* 21 (3): 117–132. https://doi.org/10.1002/(SICI)1521-3927(20000201)21:3<117::AID-MARC117>3.0.CO;2-X.

Jian, J., Z. Xiangbin, and H. Xianbo. 2020. “An Overview on Synthesis, Properties and Applications of Poly (Butylene-Adipate-Co-Terephthalate)–PBAT.” *Advanced Industrial and Engineering Polymer Research* 3 (1): 19–26. https://doi.org/10.1016/j.aiepr.2020.01.001.

Kian, L. K., M. Jawaid, M. H. Mahmoud, N. Saba, H. Fouad, O. Y. Alothman, and Z. Karim. 2022. “PBAT/PBS Blends Membranes Filled with Nanocrystalline Cellulose for Heavy Metal Ion Separation.” *Journal of Polymers and the Environment* 30 (12): 5263–5273. https://doi.org/10.1007/s10924-022-02590-3.

Krebs, F. C. 2009. “Fabrication and Processing of Polymer Solar Cells: A Review of Printing and Coating Techniques.” *Solar Energy Materials & Solar Cells* 93 (4): 394–412. https://doi.org/10.1016/j.solmat.2008.10.004.

Kumar, V., M. de la Luz Reus-Medina, and D. Yang. 2002. “Preparation, Characterization, and Tabletting Properties of a New Cellulose-Based Pharmaceutical Aid.” *International Journal of Pharmaceutics* 235 (1–2): 129–140. https://doi.org/10.1016/S0378-5173(01)00995-4.

Lang, H., X. Chen, J. Tian, J. Chen, M. Zhou, F. Lu, and S. Qian. 2022. “Effect of Microcrystalline Cellulose on the Properties of PBAT/Thermoplastic Starch Biodegradable Film with Chain Extender.” *Polymers* 14 (21): 4517. https://doi.org/10.3390/polym14214517.

Ma, X., P. R. Chang, and J. Yu. 2008. “Properties of Biodegradable Thermoplastic Pea Starch/Carboxymethyl Cellulose and Pea Starch/Microcrystalline Cellulose Composites.” *Carbohydrate Polymers* 72 (3): 369–375. https://doi.org/10.1016/j.carbpol.2007.09.002.

Ma, X., Y. Cheng, X. Qin, T. Guo, J. Deng, and X. Liu. 2017. “Hydrophilic Modification of Cellulose Nanocrystals Improves the Physicochemical Properties of Cassava Starch-Based Nanocomposite Films.” *LWT* 86:318–326. https://doi.org/10.1016/j.lwt.2017.08.012.

Mathew, A. P., K. Oksman, and M. Sain. 2005. “Mechanical Properties of Biodegradable Composites from Poly Lactic Acid (PLA) and Microcrystalline Cellulose (MCC).” *Journal of Applied Polymer Science* 97 (5): 2014–2025. https://doi.org/10.1002/app.21779.

Meraj, A., M. Jawaid, S. P. Singh, M. M. Nasef, H. Ariffin, and M. M. Haafiz. 2023. “Effect of Natural Deep Eutectic Solvents on Properties of Micro Crystalline Cellulose Isolated from Kenaf Fibre.” *Industrial Crops and Products* 203:117129. https://doi.org/10.1016/j.indcrop.2023.117129.

Mohanty, A., M. Misra, and G. Hinrichsen. 2000. “Biofibres, biodegradable polymers and biocomposites: An overview.” *Macromolecular Materials and Engineering* 276-277 (1): 1. https://doi.org/10.1002/(SICI)1439-2054(20000301)276:1<1::AID-MAME1>3.0.CO;2-W.

Nagata, M., and K. Inaki. 2011. “Biodegradable and Photocurable Multiblock Copolymers with Shape-Memory Properties from poly(ε-Caprolactone) Diol, Poly(ethylene Glycol), and 5-Cinnamoyloxyisophthalic Acid.” *Journal of Applied Polymer Science* 120 (6): 3556–3564. https://doi.org/10.1002/app.33531.

Olivato, J., M. Nobrega, C. Müller, M. Shirai, F. Yamashita, and M. Grossmann. 2013. “Mixture Design Applied for the Study of the Tartaric Acid Effect on Starch/Polyester Films.” *Carbohydrate Polymers* 92 (2): 1705–1710. https://doi.org/10.1016/j.carbpol.2012.11.024.

Pandian, H., K. Senthilkumar, M. Naveenkumar, S. Samraj, and S. S. 2023. “Azadirachta Indica Leaf Extract Mediated Silver Nanoparticles Impregnated Nano Composite Film (AgNP/MCC/Starch/Whey Protein) for Food Packaging Applications.” *Environmental Research* 216:114641. https://doi.org/10.1016/j.envres.2022.114641.

Pavia, D., G. Lampman, and G. Kriz. 2001. *Introduction to Spectroscopy, Brooks/Cole Thomson Learning. Inc*, 13–101. Washington: United Kingdom, United States.

Petersson, L., and K. Oksman. 2006. “Biopolymer Based Nanocomposites: Comparing Layered Silicates and Microcrystalline Cellulose as Nanoreinforcement.” *Composites Science and Technology* 66 (13): 2187–2196. https://doi.org/10.1016/j.compscitech.2005.12.010.

Raharjo, W. W., R. Salam, and D. Ariawan. 2023. “The Effect of Microcrystalline Cellulose on the Physical, Thermal, and Mechanical Properties of Composites Based on Cantala Fiber and Recycled High-Density Polyethylene.” *Journal of Natural Fibers* 20 (2): 2204454. https://doi.org/10.1080/15440478.2023.2204454.

Raquez, J. M., Y. Nabar, R. Narayan, and P. Dubois. 2008. “In situ Compatibilization of Maleated Thermoplastic Starch/Polyester Melt-Blends by Reactive Extrusion.” *Polymer Engineering & Science* 48 (9): 1747–1754. https://doi.org/10.1002/pen.21136.

Rasheed, M., M. Jawaid, B. Parveez, A. Hussain Bhat, and S. Alamery. 2021. “Morphology, Structural, Thermal, and Tensile Properties of Bamboo Microcrystalline Cellulose/Poly (Lactic Acid)/Poly (Butylene Succinate) Composites.” *Polymers* 13 (3): 465. https://doi.org/10.3390/polym13030465.

Reis, M. O., J. B. Olivato, J. Zanela, F. Yamashita, and M. V. E. Grossmann. 2017. “Influence of Microcrystalline Cellulose in Thermoplastic Starch/Polyester Blown Films.” *Polímeros* 27 (2): 129–135. https://doi.org/10.1590/0104-1428.2338.

Reis, M. O., J. Zanela, J. Olivato, P. S. Garcia, F. Yamashita, and M. V. E. Grossmann. 2014. “Microcrystalline Cellulose as Reinforcement in Thermoplastic Starch/Poly (Butylene Adipate-Co-Terephthalate) Films.” *Journal of Polymers and the Environment* 22 (4): 545–552. https://doi.org/10.1007/s10924-014-0674-7.

Rezwan, K., Q. Chen, J. J. Blaker, and A. R. Boccaccini. 2006. “Biodegradable and Bioactive Porous Polymer/Inorganic Composite Scaffolds for Bone Tissue Engineering.” *Biomaterials* 27 (18): 3413–3431. https://doi.org/10.1016/j.biomaterials.2006.01.039.

Sellami, F., O. Kebiche-Senhadji, S. Marais, N. Couvrat, and K. Fatyeyeva. 2019. “Polymer Inclusion Membranes Based on CTA/PBAT Blend Containing Aliquat 336 as Extractant for Removal of Cr (VI): Efficiency, Stability and Selectivity.” *Reactive & Functional Polymers* 139:120–132. https://doi.org/10.1016/j.reactfunctpolym.2019.03.014.

Sinsukudomchai, P., D. Aht-Ong, K. Honda, S. C. Napathorn, and M. Koller. 2023. “Green Composites Made of Polyhydroxybutyrate and Long-Chain Fatty Acid Esterified Microcrystalline Cellulose from Pineapple Leaf.” *PLOS ONE* 18 (3): e0282311. https://doi.org/10.1371/journal.pone.0282311.

Siracusa, V., P. Rocculi, S. Romani, and M. Dalla Rosa. 2008. “Biodegradable Polymers for Food Packaging: A Review.” *Trends in Food Science & Technology* 19 (12): 634–643. https://doi.org/10.1016/j.tifs.2008.07.003.

Stuart, M. A. C., W. T. Huck, J. Genzer, M. Müller, C. Ober, M. Stamm, G. B. Sukhorukov, et al. 2010. “Emerging Applications of Stimuli-Responsive Polymer Materials.” *Nature Materials* 9 (2): 101–113. https://doi.org/10.1038/nmat2614.

Sun, X., C. Lu, Y. Liu, W. Zhang, and X. Zhang. 2014. “Melt-Processed Poly (Vinyl Alcohol) Composites Filled with Microcrystalline Cellulose from Waste Cotton Fabrics.” *Carbohydrate Polymers* 101:642–649. https://doi.org/10.1016/j.carbpol.2013.09.088.

Tchmutin, I., N. Ryvkina, N. Saha, and P. Saha. 2004. “Study on Biodegradability of Protein Filled Polymer Composites Using Dielectric Measurements.” *Polymer Degradation & Stability* 86 (3): 411–417. https://doi.org/10.1016/j.polymdegradstab.2004.05.012.

Tessema, T. A., A. T. Feroche, G. A. Workneh, and T. Gabriel. 2023. “Physicochemical Characterization of Cellulose and Microcrystalline Cellulose from Cordia Africana Lam. Seeds.” *Journal of Natural Fibers* 20 (2): 2198278. https://doi.org/10.1080/15440478.2023.2198278.

Vargas Ferreira, F., L. De Simone Cividanes, F. Sales Brito, B. Rossi Canuto de Menezes, W. Franceschi, E. Nunes Simonetti, and G. Patrocnio Thim. 2016. “Functionalizing Graphene and Carbon Nanotubes.” In *Switzerland AG*, Springer International Publishing. https://doi.org/10.1007/978/-3-319-35110-0.

Wang, K. H., T. M. Wu, Y. F. Shih, and C. M. Huang. 2008. “Water Bamboo Husk Reinforced Poly (Lactic Acid) Green Composites.” *Polymer Engineering & Science* 48 (9): 1833–1839. https://doi.org/10.1002/pen.21151.

Wu, C.-S. 2012. “Characterization of Cellulose Acetate-Reinforced Aliphatic–Aromatic Copolyester Composites.” *Carbohydrate Polymers* 87 (2): 1249–1256. https://doi.org/10.1016/j.carbpol.2011.09.009.

Zuo, J., T.-S. Chung, G. S. O’Brien, and W. Kosar. 2017. “Hydrophobic/Hydrophilic PVDF/Ultem® Dual-Layer Hollow Fiber Membranes with Enhanced Mechanical Properties for Vacuum Membrane Distillation.” *Journal of Membrane Science* 523:103–110. https://doi.org/10.1016/j.memsci.2016.09.030.